Philosophical Magazine
2010, 1–11, iFirst

Taylor & Francis
Taylor & Francis Group

Development of band patterns in surface films: A simple theory

N.H. Fletcher*

Department of Electronic Materials Engineering Research School of Physics and Engineering, Australian National University, Canberra 0200, Australia

(*Received 10 January 2010; final version received 13 June 2010*)

Semiconductor technology often employs thin films deposited on crystal surfaces, and in some cases these films can self-organize into band, ring or spiral patterns during annealing. A simple theory is proposed which predicts the stability or instability of such films and, in the case of instability, the band spacing, which depends upon bulk, surface and interfacial free energies. This information could be of use in self-assembly techniques. In some cases, bands condense into particle arrays upon further annealing, and a theoretical model is developed to predict the subsequent evolution of circular band patterns by diffusion, which causes the regular disappearance of alternate bands.

Keywords: band patterns; thin films; Ostwald ripening; rings; surface diffusion; nanoparticles

1. Introduction

Many semiconductor devices rely upon the deposition of a thin film upon a semiconductor substrate and the subsequent shaping of this film into patterned structures using a 'top down' fabrication technique. Another approach that shows increasing promise is to have the film self-assemble into the required pattern using a 'bottom up' technique. In the first case, it is essential that the shape of the film be stable over time, while the second technique relies upon an inherent instability on the film to generate the desired pattern. There is therefore increasing interest in understanding the mechanisms controlling stability and pattern growth in thin films.

The whole matter of pattern generation is, of course, significant in many areas of physics and biology, as has been summarized by Levin and Segel [1]. Many different physical processes can be involved and the resulting patterns may be either regular or chaotic. Much of the underlying theory of pattern development in thin layers was developed a long time ago by Cahn and Hilliard [2–4] who derived a compact nonlinear equation to describe the time evolution of an unstable mixed system separating into two components. In the case of regular rather than chaotic patterns, one generally successful approach is to assume a possible pattern with adjustable parameters and to calculate its development rate as a function of these parameters.

*Email: neville.fletcher@anu.edu.au

ISSN 1478–6435 print/ISSN 1478–6443 online

DOI: 10.1080/14786435.2010.502147
http://www.informaworld.com

The parameter set that gives the fastest initial growth rate is then likely to be the one that finally emerges.

An example of such a system related to semiconductor devices is a recent study of the development of spiral patterns of gold nanoparticles on the surface of a gold-implanted silicon wafer when it is subsequently annealed [5,6]. The implanted gold atoms are localized in a layer about 25 nm in thickness where they form an alloy with the silicon. If the implanted wafer is then annealed for a time as short as 5 seconds at a temperature of 650°C, then a pattern of closely spaced bands with alternating high and low gold content begins to develop on the surface, a typical spacing being about 10 μm. These bands are themselves generally organized into larger patterns so that they form circles or spirals about particular points on the surface or sometimes less symmetrical patterns. As the annealing time is increased above about 100 seconds at this temperature the gold-rich bands condense into arrays of particles up to about 1 μm in diameter. As the annealing time is increased some of the bands begin to disappear in an almost alternating sequence beginning near the pattern center. Similar behavior has been observed with other metallic films on silicon.

The present paper produces a semi-quantitative theoretical explanation of the development of such band structures and the dependence of the band spacing upon critical parameters such as film thickness and both surface and bulk free energies. The second stage of the annealing development is then explored for the simplified case of circular ring patterns, with particle nucleation followed by diffusive Ostwald ripening leading to a modification of the ring spacing around a central particle. Although no specific parameter values are investigated, the results indicate how the relative values of the parameters must be chosen in order to achieve the contrasting aims of a stable film or a film that will develop some form of self-assembled pattern.

2. Formation of band patterns

As the simplest case, consider a uniform substrate upon which is a thin film of binary alloy which has a melting point much lower than that of the substrate. When the film is melted during annealing there is the possibility of a compositional instability developing if this lowers the free energy per unit area. To treat this simplest possible case, let us examine the possibility that a layer with initial composition AB gradually breaks into uniform bands of alternating compositions A and B under the influence of some forcing function. If there is some particular separation for which the bands develop most rapidly, then this is likely to be the dominant instability that occurs and it will define the final pattern.

Following the usual method for analysing instabilities, suppose that there is an initially sinusoidal perturbation of the composition $A_{1+c}B_{1-c}$ of the surface film of the form

$$c = \tanh(\alpha \sin kx), \tag{1}$$

where α is a numerical parameter that increases with time, thus quantifying the degree of compositional separation, x is a coordinate in the surface plane, and $k = 2\pi/w$ where w is the repeat spacing of bands normal to the x-direction. The hyperbolic tangent function ensures separation into pure bands of composition

A and B as $\alpha \to \infty$, while the approximation $c \approx \alpha \sin kx$ is appropriate for examination of the initial stages of pattern, development which control the final outcome. In the case of circular patterns, it is appropriate to use a Bessel function perturbation of the form $c = \tanh(\alpha J_0(kr))$ or even the simpler $c = \cos kr$, both of which approximate parallel bands at large radius. The analysis is then similar to that for the simpler sinusoidal case but will not be examined in detail here.

This small perturbation (1) then leads to variation in three significant physical properties of the layer. First, there will be a change in the average bulk free energy G per unit area of the film. If G_{AB} is the free energy per unit volume of the original eutectic film, and G_A and G_B the free energies of the two completely separated phases, then we can assume the approximation

$$G(c) = G_{AB} + a_1 c + a_2 c^2 + a_3 c^3 \tag{2}$$

for the bulk free energy of the composition $A_{1+c}B_{1-c}$. The fact that, in the present case, AB is a eutectic so that G_{AB} is a minimum is not for the moment important. Applying this expression to the cases $c = \pm 1$ then gives

$$a_2 = \frac{G_A + G_B}{2} - G_{AB}. \tag{3}$$

A small variation c away from the AB composition into two complementary phases $A_{1+c}B_{1-c}$ and $A_{1-c}B_{1+c}$ and summation of their separate free energies then leads to cancellation of the odd terms in (2) and changes the free energy per unit area of film by an amount

$$\delta G \approx c^2 h \left(\frac{G_A + G_B}{2} - G_{AB} \right), \tag{4}$$

where h is the film thickness.

Secondly there will be a change in the average free energy σ per unit area of the interface between the film and the substrate, together with that of the film free surface, of the form

$$\delta\sigma = \frac{c^2}{2} \left(\frac{\sigma_A + \sigma_B}{2} - \sigma_{AB} \right), \tag{5}$$

where the subscripts have the same meaning as in (4) and terms linear in c cancel for the same reason.

The third contribution to the total free energy arises from the composition gradient within the film. This question was examined in detail by Cahn and Hilliard [2] and the conclusion, as expressed in their equation (2.14) and the following unnumbered equation, is that the free energy per unit area of such a single composition interface is given by

$$\sigma_I = 2N\kappa \int_{-\infty}^{+\infty} (dc/dx)^2 dx \to 2N\kappa \int_{-w/2}^{+w/2} (dc/dx)^2 dx \tag{6}$$

where N is the number of atoms per unit volume, c is the relative concentration of one of the phases which behaves as in (1), and κ is a constant proportional to the 'gradient energy' of the composition transition. For a banded transition pattern a good approximation for $c(x)$ is that given by (1), and the free energy for a single band

interface is then obtained by limiting the integral range to $-\pi/2k < x < +\pi/2k$, as shown to the right in (6), and multiplying by the film thickness h. The result for the free energy σ per unit length of internal film interface is then

$$I = \frac{\alpha^2 \sigma_I h}{2w}. \tag{7}$$

Note that this expression gives the expected result $I \to \sigma_I h/2w$ in the limit $\alpha \gg 1$, if the accurate expression (1) is used, implying complete phase separation.

The total free energy per unit area of film driving the formation of bands is thus

$$E = -(\delta G + \delta\sigma + I). \tag{8}$$

This driving energy is distributed along a total band length $1/w$ per unit area of film, giving a driving energy Ew per unit length of band so that the energy gradient, or driving force, normal to the band edge is simply proportional to E. Since the amount of material to be transported to unit length of an individual band is proportional to $wh|\alpha|$, the rate of generation of bands is

$$R(w) \propto \frac{E}{wh|\alpha|} = \left(Wh + X - Y\frac{h}{w}\right)\frac{|\alpha|}{2wh}, \tag{9}$$

where

$$W = G_{AB} - \frac{G_A + G_B}{2}, \quad X = \sigma_{AB} - \frac{\sigma_A + \sigma_B}{2}, \quad Y = \sigma_I. \tag{10}$$

It is clear from (4)–(9) above that the initial state $\alpha = 0$ may be either stable or metastable and that bands will form only if $R > 0$, which puts constraints upon the physical parameters W, X and Y defined in (10). If $R > 0$ then the dominant band pattern growth will be that for which $R(w)$ is greatest. Applying the condition $\partial R/\partial w = 0$ to Equation (9) then gives

$$w = \frac{2Yh}{X + Wh} \tag{11}$$

for the width parameter of the most rapidly developing band structure.

Since the interface free energy Y between the separated bands is necessarily positive, bands will develop only if $X + Wh > 0$. There are then three possibilities, which have been simply illustrated in Figure 1 with h measured in terms of $h_0 = |X/W|$ and w in terms of $w_0 = |2Y/W|$, which is generally much larger.

(a) If $X > 0$ so that substrate interface energy is a driving force, and $W > 0$ so that the separated phases are stable relative to the initial mixed phase, then the band separation w is proportional to the film thickness h for thin films but reaches a maximum value of $2Y/W$ for very thick layers, as shown in curve (a) of Figure 1.

(b) If $X > 0$ but $W < 0$ so that surface energy is the driving force and the separated A and B phases are less stable than the original AB phase, then w is proportional to the film thickness h for very thin films but increases to

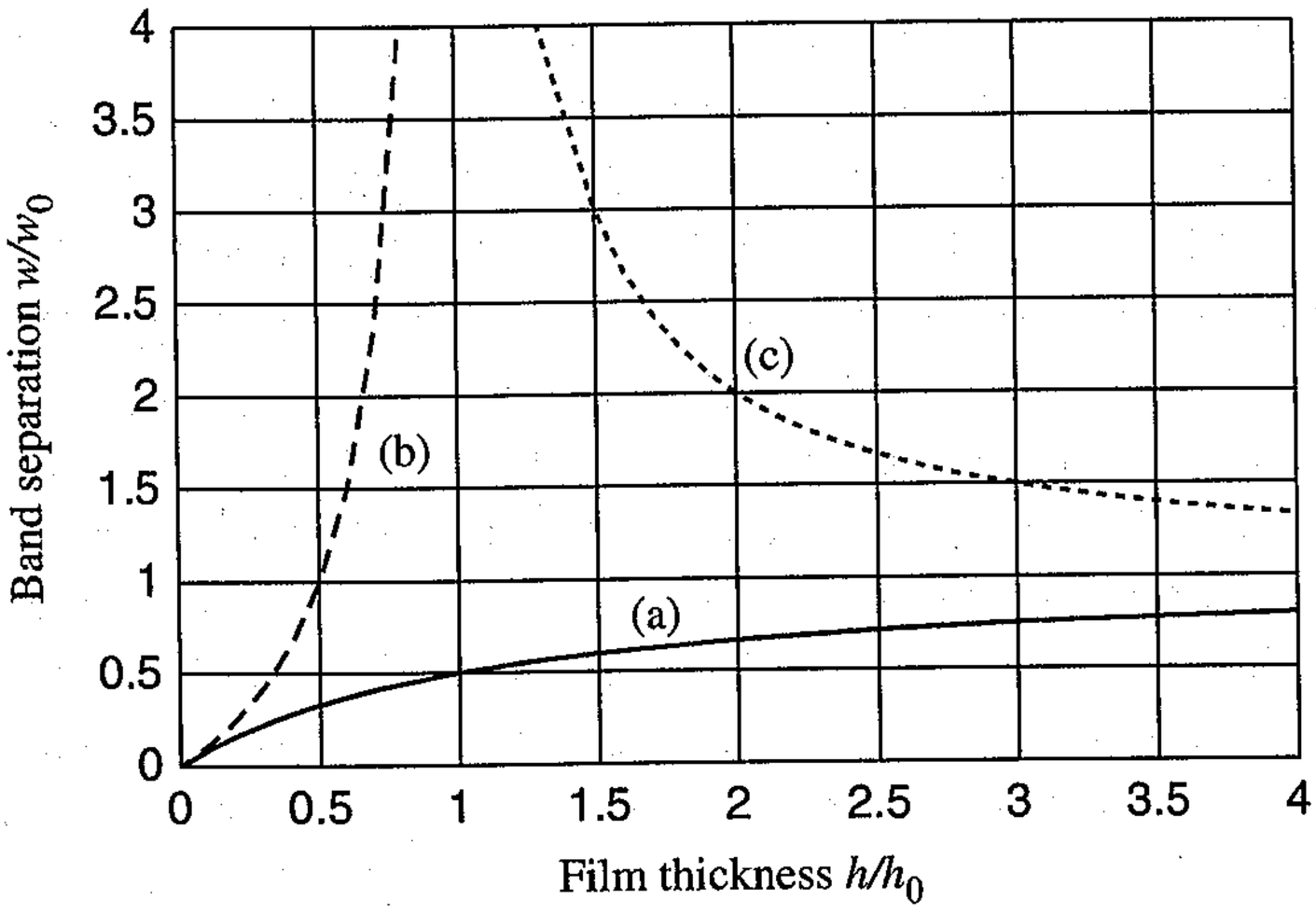

Figure 1. Variation of band separation w with film thickness h for the three possible sign combinations of the parameters X and W defined in (10): (a) $X>0$, $W>0$, (b) $X>0$, $W<0$, (c) $X<0$, $W>0$. Parameters are normalized in terms of $h_0=|X/W|$ and $w_0=|2Y/W|$, which is generally much larger.

infinity for $h=-X/W$ so that no bands develop in films thicker than this, as shown in curve (b).

(c) If $X<0$ and $W>0$ so that bulk free energy is the driving force, then no bands develop for $h<-X/W$ but bands do develop in thicker films and these reach a limiting separation $-2Y/W$ for very thick layers, as shown in curve (c).

(d) If $X<0$ and $W<0$ then no bands develop.

3. Formation of circular and spiral patterns

While a uniform pattern of straight bands is simplest to model, it is not a situation that normally occurs to any good approximation. Instead bands usually form spiral patterns which then interact with one another to produce 'swirling' structures [5]. It is interesting to see how these patterns might be produced, though it should be noted that away from the pattern center the structure is well approximated by simple parallel bands.

Instead of investigating the development of a sinusoidal parallel-band pattern, the obvious trial function in this case is a Bessel function $J_0(kr)$ which appropriately satisfies the equation $\nabla^2 c+k^2 c=0$ in plane polar coordinates, in analogy with the use of $\sin(kx)$ as the solution of $\partial^2 c/\partial x^2+k^2 c=0$ for the development of parallel bands. At large radial distances $J_0(kr)\approx[2/(\pi kr)]^{1/2}\cos(kr-\pi/4)$ so that we might expect the band separation to be similar to that predicted above for the linear case, but interest concentrates on behavior near the origin where $J_0\to 1$. Even here things are fairly straightforward, for the maxima and minima of $J_0(kr)$ follow a nearly equally spaced sequence except that the initial circle centered at $r=0$ has a radius $r=2.4/k$ which is rather greater than the half width $1.6/k$ of the next band, though

the integrated value of $J_0(kr)$ over the band is almost the same. This larger central area should show up in the resulting ring pattern, as indeed it does [5].

The fact that circular patterns are hardly ever observed, but only spirals, is interesting and appears to have a subtle explanation. The development of either circular or spiral patterns requires the presence of some irregularity, or at least a random nucleation point, to define the center of the pattern. In practice this irregularity may be in the shape of a nanoparticle deposited during the initial processing or may be the location of surrounding band patterns. If the pattern is centered on some such irregularity that is not perfectly circular, then growth of bands may be expected to begin at some point near the nucleus and to proceed in a nearly circular manner around it but, because of the lack of exact circular symmetry, the two ends of the growing band will approach each other from positions at slightly different distances from the pattern center. Because of diffusive flow to the growing band ends they will effectively repel each other, so that one is directed inwards towards the center and the other outwards, initiating a spiral pattern. An explanation similar to this has been applied to some of the pattern developments in Liesegang rings by Krug and Brandtstädter [7].

4. Comparison with experiment

Predictions for band development in real systems can in principle be obtained from (11) by inserting numerical values for the free energy parameters W, X, Y and the film thickness h. Unfortunately, such physical quantities are not easy to determine and are not generally available in the literature, but some estimates can be made. The bulk free energies G in the definition of W are typically of order 10^8 J/m^3 while the surface free energies σ in the definition of X and Y are typically of order 10 J/m^2. If the fractional difference of these quantities for the mixed material AB from the average of the quantity for A and B separately is the same in each case, then this suggests that $X/W \sim 10^{-7}$ m and $Y/W \sim 10^{-6}$ m. The transition point at $h=1$ in Figure 1 is therefore expected to occur at a film thickness of order $2Y/W \sim 2\,\mu$m.

The experiments of Venkatachalam et al. [5] used films prepared by implanting gold into a silicon substrate. The implanted gold dose was about $1\text{–}4 \times 10^{20}$ m^{-2} and this was localized in a surface layer about 20 nm in thickness, giving an alloy of about 30–80% gold in silicon. The implant dose for the specimens studied in detail gave a gold fraction of 58% which is not too far from the AB alloy assumed in our calculations. The resulting ring separation in the initial stages of annealing was about 5 μm, so that $w/h \approx 250$. This is significantly larger than the order-of-magnitude prediction $w/h = 2Y/X \sim 20$ derived from the analysis, but this predicted value is itself based on order-of-magnitude estimates of the free energy ratios involved and so is very uncertain, so that the agreement between theory and experiment is as good as can be expected. From the discussion in the previous paragraph, the critical point $h=1$ corresponds to a film thickness of about 2 μm, so that the experimental results are for the region near $h=0.01$ in Figure 1 and either of the alternatives (a) or (b) might apply.

Unfortunately, the experimental data is confined to implants with the same extraction potential of 10 keV, so that the thickness of the deposited gold film was

not changed. It was found that ring patterns appeared over only a limited range of implant times and thus of gold concentrations, which is to be expected because too little or too much gold will move the composition away from the assumed AB value and decrease the driving energies X and Y, which must be generalized from (10) to allow for the different A/B ratio. The conclusion from the limited available experimental data is therefore that the theory provides a reasonable approximation to the observed data, given the extent of the unknown quantities involved, but that more extensive experiments are required to distinguish between the alternatives (a) and (b) of Figure 1.

On a larger scale, the analysis leading to Figure 1 can be applied to many other cases in which thicker layers are deposited on substrates and subsequently decompose into bands. The critical point $h=1$ on the diagram, as noted above, could be reached with films of order just a few micrometres in thickness, and thus applies in many practical cases.

5. Ostwald ripening of the rings

Once the surface film has separated into bands, rings, or more complex structures as described above, several alternative developments are possible. In the simplest case, nothing more happens except that the bands develop well-defined edges, as described by the tanh function of (1) for large α. In other cases, such as that studied by Venkatachalam et al. [5,6], the bands of major composition A, silicon in this case, may be compatible with the substrate while those of major composition B, gold in this case, are not. During the annealing process the B-rich bands condense into arrays of particles, the spacing between these particles being almost uniform rather than random. This occurs through a process of either homogeneous nucleation or of heterogeneous nucleation on the uniform substrate surface, the physics of each process being well known [8,9] and summarized in a more recent publication [10]. The nucleation rate R_N for these particles is a very strong function of the saturation ratio $s=c/c_\infty$, varying as

$$R_N = K\exp[-\gamma/(\ln s)^2], \tag{12}$$

where K is a very large number and γ is another constant. When one particle is nucleated, the diffusion depletion field established around it ensures that no other particle will nucleate in its immediate vicinity. This also ensures that all the particles in the rings have very similar sizes and are nearly equally spaced. Details of this nucleation process need not concern us here.

In the case of surface layers that have developed a ring or spiral structure, there is usually, however, something different about the particles in the circle around the origin – the first positive segment of the Bessel function $J_0(kr)$ – making them rather larger than the other particles, or there may even be a single large particle at the center of this cluster responsible for its circular shape. The interest now is to compute how this set of particle rings develops during the annealing process.

For simplicity we consider the case where there is a single larger particle at the origin, but this could be replaced by a disc-like array of larger-than-average particles as might arise from occurrence of the Bessel-function initial perturbation.

Let r be the radial coordinate centered on the larger particle at the origin, then the properties and behavior of particles within a given ring are taken to all be the same, each particle in the ring having radius $a(r, t)$ at time t.

First we need to calculate the solute concentration near a particle of radius a. Let the equilibrium solute concentration on the substrate surface at the temperature of interest be c_∞, and suppose the equilibrium surface concentration close to a particle of radius a is c_a. The particle shape may be complex but we take it to be a simple spherical dome, details of the geometry being determined by the contact angle on the substrate and thus by the surface and interfacial free energies involved. Since the total free energy of the particle has a volume component that varies as a^3 and a surface component that varies as a^2, it can be shown [10] that

$$c_a = c_\infty e^{\beta/a}, \tag{13}$$

where β is a calculable numerical parameter proportional to surface free energy. This is a version of the classical Gibbs–Thomson formula.

If the angular variation of solute concentration c is assumed to be zero, as in the simple models discussed here, then the steady-state diffusion equation for free space in two dimensions has the form $\nabla^2 c = 0$, which becomes $r\partial c/\partial r = P$ where r is the radial coordinate and P is a constant. The diffusion field between rings r_1 and r_2 then has the form

$$c(r) = P \ln r + Q, \tag{14}$$

where Q is another constant and r_2 is the ring closest to r_1 that still has a non-zero particle size. Both positive and negative values of $r_2 - r_1$ must be considered, and the calculations for these two cases do not interfere since the two domains are separated by the ring at r_1. Matching this result to the equilibrium solute concentrations $c(r_1)$ and $c(r_2)$ at rings r_1 and r_2 as given by (13) then gives

$$P = \frac{c(r_2) - c(r_1)}{\ln r_2 - \ln r_1} \tag{15}$$

$$Q = \frac{c(r_1) \ln r_2 - c(r_2) \ln r_1}{\ln r_2 - \ln r_1}. \tag{16}$$

The diffusion flow in the film towards the smaller of the two rings is therefore

$$2\pi r D \frac{\mathrm{d}c(r)}{\mathrm{d}r} = 2\pi D P, \tag{17}$$

where D is the diffusion coefficient of the solute atoms. The rate at which the total gold content C of the r_1 ring changes is then

$$\frac{\mathrm{d}C}{\mathrm{d}t} = 2\pi D(P_+ - P_-), \tag{18}$$

where P_+ is the value of P evaluated from (15) for the neighboring larger ring that still exists, and P_- is the value of P for the neighboring smaller ring. Note that $\mathrm{d}C/\mathrm{d}t$ may be either positive or negative, corresponding to inward or outward radial diffusion on the substrate surface.

Suppose each ring contains ν particles per unit area, so that the ring at position r contains $\pi r w \nu$ particles each of radius a. Equation (18) is then equivalent to the statement

$$\frac{\mathrm{d}a}{\mathrm{d}t} = \frac{\mu D}{r a^2 w \nu}(P_+ - P_-), \tag{19}$$

where μ is a numerical parameter of order unity, the value of which depends upon the particle shape, and thus upon the contact angle of the particle material on the substrate. If there is just a single larger particle at the origin then there is an anomaly, since its nominal ring radius is zero and $P_- = 0$. The appropriate approximation is therefore to set $r = a_0$ for this particle and to update this for each time step in the numerical integration process. The parameter D simply specifies the overall rate of the diffusion process.

Equations (13), (15) and (19), together with initial conditions on particle size in the rings and at the origin now provide a sufficient basis for numerical calculation of the evolution of the particle sizes in the rings spanning the field. The first thing to happen is that the innermost ring #1 loses content by diffusion to the central particle. This causes the particles in the ring to become smaller in size, which increases their equilibrium solute concentration and causes them to lose material ever more rapidly. Because, however, the particles in the next ring #2 are shielded by ring #1, they increase in size by diffusion from the particles in ring #1. This increase in particle size also means that the ring #2 particles are larger than those in ring #3, so that they grow a little more at the expense of this ring as well. This process propagates through the ring system, though with its effect decreasing with increasing radial distance, and leads to the progressive vanishing of alternate rings, with the process being more rapid for rings near the origin than for distant rings which are more stable.

While an analytical solution for even a finite number of rings is almost impossible, a numerical simulation of this process is straightforward, since over the small time interval of each step the particle size in each ring can be taken as constant, the rate of change calculated, and all the particle sizes updated after each step. The result of such a numerical calculation is given in Figure 2, which plots the evolution of particle size with time for a ring system with a single larger particle, initially with twice the radius of the other particles, at the origin. The other parameter values were $a_0 = 0.4$, $a_i = 0.2$ for $i \geq 1$, $c_\infty = 0.01$, $\beta = 0.1$ and $D = 1/2\pi$.

6. Comparison with experiment

This predicted behavior is seen in Figure 5c of the paper by Venkatachalam et al. [5] and shows all the features predicted by this analysis, particularly the progressive vanishing of bands near the center of the pattern, where there is a large particle that has presumably initiated ring formation. This figure also shows that the particles in the inner rings have grown in size relative to those in the outer rings, as predicted in our analysis. Figure 5b of that paper shows the way in which rings or spirals growing around different particles interact by competitive diffusion. This is, however, clearly a complicated process to analyse.

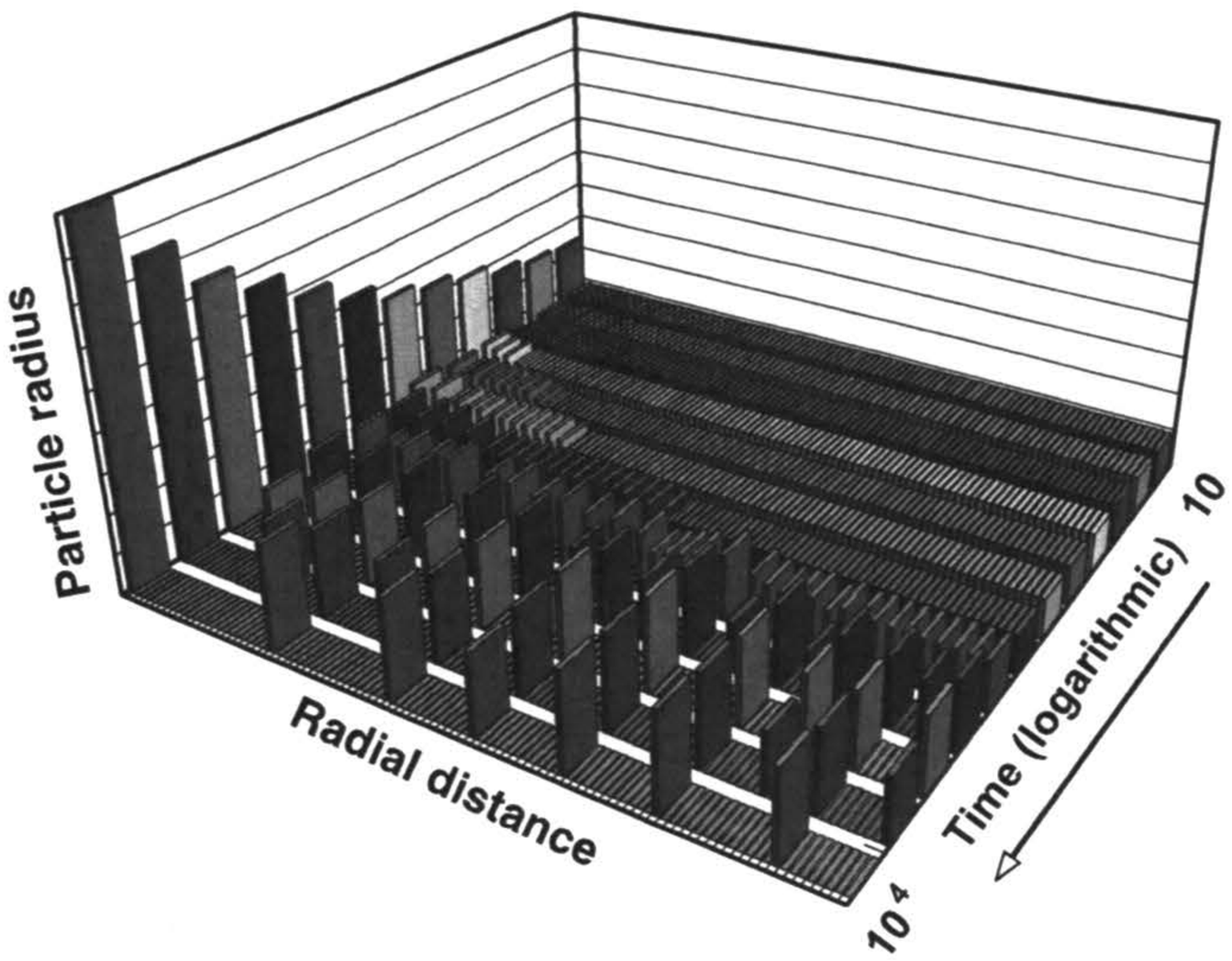

Figure 2. Calculated evolution of particle size in initially uniform rings as a function of time and distance from a larger particle at the origin. The particle at the origin, on the left in the figure, was initially twice the radius of the other particles, and its steadily increasing radius is plotted at the left of the figure. The particles in the rings either disappear or else increase in radius with annealing time.

7. Conclusions

The development of patterns of bands, spirals, and even more complex structures, during the annealing of thin metastable alloy films deposited on planar surfaces has been shown to arise from the existence of many possible instabilities, one of which becomes dominant because it develops most rapidly in its early stages. The resulting patterns will always have complex structures because simple patterns begin to develop nearly simultaneously in many locations on the film and the interaction of these patterns causes complex deviations from simple geometries.

The theory set out above is admittedly only semi-quantitative, but this has advantages as well as disadvantages. While the theory does not yet provide any precise numerical predictions for some specific system that can be checked experimentally, the advantage is that it describes a broad range of systems and shows how the observed outcomes can be explained at least qualitatively, and perhaps semi-quantitatively, in terms of a small number of physical parameters with clear meanings, such as layer thickness and interface free energy. The predictions of the theory may therefore prove of assistance in devising experiments that give greater insight into this interesting field, and ultimately for complex semiconductor device fabrication techniques.

References

[1] S.A. Levin and L.A. Segel, SIAM Rev. 27 (1985) p.45.
[2] J.W. Cahn and J.E. Hilliard, J. Chem. Phys. 28 (1958) p.258.
[3] J.W. Cahn, J. Chem. Phys. 30 (1959) p.1121.
[4] E.W. Hart, Phys. Rev. 113 (1959) p.412.

[5] D.K. Venkatachalam, D.K. Sood and S.K. Bhargava, Nanotechnology 19 (2008) p.015605.
[6] D.K Venkatachalam, N.H. Fletcher, D.K. Sood and R.G. Elliman, Appl. Phys. Lett. 94 (2009) p.213110.
[7] H.-J. Krug and H. Brandtstädter, J. Phys. Chem. A. 103 (1999) p.7811.
[8] J. Frenkel, J. Chem. Phys. 7 (1939) p.538.
[9] M. Volmer, *Kinetik der Phasenbildung*, Steinkopff, Dresden and Leipzig, 1939.
[10] N.H. Fletcher, *The Physics of Rainclouds*, Cambridge University Press, Cambridge, 1962, Ch. 3.